PROCEEDINGS OF SCIENCE

Diffuse supernova neutrino background as a probe to explore the fate of stellar core collapse

Yosuke Ashida[1]*, **Ken'ichiro Nakazato**[2] **and Takuji Tsujimoto**[3]
E-mail: yosuke.ashida@icecube.wisc.edu

A diffuse flux of neutrinos emitted from all the past core collapses of massive stars, the diffuse supernova neutrino background (DSNB), still remains undiscovered; however, new generation detectors for the next decades expect to detect DSNB for the first time. This is expected to bring the stage of core collapse studies to the next level and therefore elaborate preparations are required to make statements on physics with observed results. In this study, the fact that the neutrino spectrum changes for different fates of stellar core collapse is focused and the frequencies of successful and failed supernovae are deduced to be as a function of redshift by connecting two evolutions of the galaxy and Universe. The calculated DSNB $\bar{\nu}_e$ flux shows unique spectral features compared to previous theoretical models at high and low neutrino energies. The new model is then tested regarding its detectability and physics model discrimination potential at water Cherenkov detectors.

[1] *Department of Physics and Astronomy, University of Utah*
[2] *Faculty of Arts and Science, Kyushu University*
[3] *National Astronomical Observatory of Japan*

* Presenter

The 38th International Cosmic Ray Conference (ICRC2023)
26 July – 3 August, 2023
Nagoya, Japan

PoS(ICRC2023)981

1. Introduction

One of the endings that massive stars with $>8M_\odot$ follow is gravitational collapse of their core, which eventually leaves a neutron star (NS) or a black hole (BH). In a successful explosive collapse, as known as core-collapse supernovae (CCSNe), plenty of materials are dispersed in the Universe, therefore it is a key factor in the context of galactic chemical evolution. Multimessenger approaches have been attempted to study stellar core collapse and among them is detecting thermal neutrinos emitted through the process by which physics in a deep stellar core is accessible. In particular, the accumulated flux of neutrinos that have arisen from core-collapse stars over the cosmic history is referred to as the diffuse supernova neutrino background (DSNB) and considered to be a unique measure of examining collapsing stars as well as the cosmic evolution. Huge theoretical and experimental efforts on the DSNB study have been made for the past few decades (see recent reviews [1, 2] and references therein); however, its observation has yet to be achieved to date. The stringent upper limits on the DSNB $\bar{\nu}_e$ flux have been extracted from the searches performed at Super-Kamiokande (SK) [3] and KamLAND [4].

In our recent work [5], the fate of stellar core collapse is focused and potential capability of DSNB measurement to access such information is discussed. Here, it is assumed that core collapse of massive stars should take either of three fates: a canonical- or high-mass NS from a successful explosion (baryonic mass of $1.47M_\odot$ or $1.86M_\odot$ respectively), or a BH from a failed-SN. For each case the DSNB $\bar{\nu}_e$ flux is calculated and this has been performed with different assumptions on the nuclear equation of state (EOS) and neutrino mass hierarchy (normal or inverted). In Ref. [5], the fluxes from these three cases are mixed with fractional parameters, $f_{\rm HNS}$ (a fraction of SNe with a high-mass NS to the total number of SNe with an NS) and $f_{\rm BH}$ (a fraction of failed-SNe to the total number of stellar core collapses), and then the experimental sensitivities at gadolinium-loaded SK (SK-Gd) and Hyper-Kamiokande (HK) to these factors are estimated. One example result from this study is shown in Figure 1.

Although the fraction of BH formation after core collapses is taken as a free parameter in Ref. [5], successful explosions are favored only for progenitors with $<18M_\odot$ from both theoretical and experimental studies. Starting with this point, a novel galactic chemical evolution model is proposed in Ref. [6], where failed-SNe forming a BH are assumed for all progenitors with $>18M_\odot$ and the initial mass function (IMF) of progenitors is considered to be galaxy-dependent (referred to as GDIMF in this work). This new model leads to unique features in the resulting DSNB flux, descriptions of which are the main scope of this article. Many descriptions in the following part are taken from our recent paper [7].

2. Modeling

In this study, galaxies are classified into five types: spheroids (E/S0), and four classes of spiral galaxies (Sab, Sbc, Scd, and Sdm). The Salpeter IMF with a slope index of a power law being $x = -1.35$ is used for the late-type galaxies (Sbc, Scd, and Sdm), while the flat IMF with $x = -0.9$ is adopted for the early-type galaxies (E/S0 and Sab) to estimate the rate of CCSNe with masses of 8–$18M_\odot$. The BH formation rate is estimated similarly but for progenitors with 18–$100M_\odot$. Here, two forms of the star formation rate (SFR), HB06 [8] and MD14 [9], are considered. In

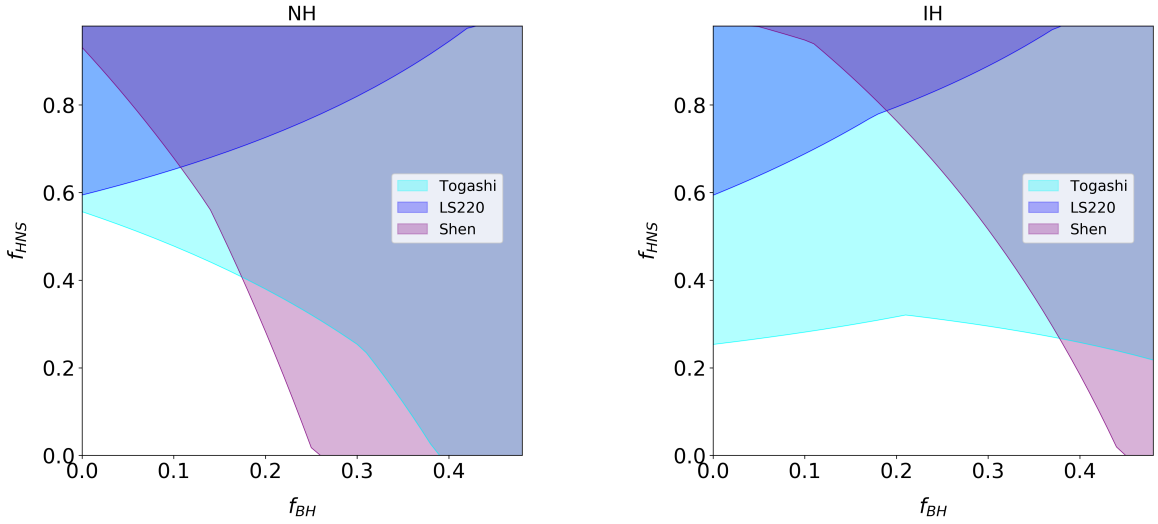

Figure 1: Detectable areas on the $f_{\rm BH}$–$f_{\rm HNS}$ plane from a 10-year operation of SK-Gd for different nuclear EOS and neutrino mass hierarchy (normal and inverted in left and right, respectively). These figures are taken from Ref. [5].

addition, three alternative assumptions are tested with different choices of IMF and BH formation for a comparison purpose as summarized in Table 1.

Table 1: Summary of the DSNB models in the present study (GDIMF-wBH is a reference model).

Model name	IMF form	BH treatment
GDIMF-wBH (ref.)	Galaxy-dependent	BHs for 18–100$M_\odot$
GDIMF-noBH	Galaxy-dependent	No BH
SalIMF-wBH	Salpeter	BHs for 18–100$M_\odot$
SalIMF-noBH	Salpeter	No BH

The DSNB flux is calculated by summing up the emitted neutrino spectra from CCSNe and failed-SNe over the redshift being 0 to 5 with a cosmological correction as,

$$\frac{d\Phi(E_\nu)}{dE_\nu} = c\int_0^5 \frac{dz}{H_0\sqrt{\Omega_{\rm m}(1+z)^3+\Omega_\Lambda}} \times \left[R_{\rm CCSN}(z)\frac{dN_{\rm CCSN}(E'_\nu)}{dE'_\nu} + R_{\rm BH}(z)\frac{dN_{\rm BH}(E'_\nu)}{dE'_\nu}\right],$$

where c is the speed of light, and $\Omega_{\rm m} = 0.3089$, $\Omega_\Lambda = 0.6911$, and $H_0 = 67.74$ km sec^{-1} Mpc^{-1} are the cosmological constants. E'_ν is the neutrino energy at an emitter with a redshift z and related to the neutrino energy at a detector on Earth E_ν via $E'_\nu = E_\nu(1+z)$. The rate of and neutrino spectrum from CCSNe are denoted as $R_{\rm CCSN}(z)$ and $dN_{\rm CCSN}(E'_\nu)/dE'_\nu$, respectively. The corresponding ones for failed-SNe forming a BH are $R_{\rm BH}(z)$ and $dN_{\rm BH}(E'_\nu)/dE'_\nu$, respectively. Three types of the nuclear EOS, Togashi [10], LS220 [11], and Shen [12], are considered in this study. In the successful explosion case, the total energy of neutrinos is larger for the nuclear EOS with a smaller

NS radius (the radius is Togashi < LS220 < Shen). In contrast, in the BH formation case, the total energy of neutrinos is larger for the nuclear EOS with a higher maximum mass of NS (the maximum mass is Shen > Togashi > LS220). See Refs. [5, 7, 13, 14] and references therein for further details. Finally, the neutrino oscillation effect is taken into account. Here, both of the normal (NH) and inverted hierarchy (IH) cases are investigated.

Figure 2 shows the resulting DSNB $\bar{\nu}_e$ flux in comparison with previous theoretical predictions and the latest experimental upper bounds. The current model observes enhancements at high and low neutrino energies compared to other models. The high energy enhancement is caused by a large contribution from failed-SNe forming a BH which this study considers for all progenitors with $>18M_\odot$. On the other hand, the low energy side below ~10 MeV is elevated because of the neutrinos redshifted from $z > 1$ in which the core-collapse rate is higher for a large contribution from the early-type galaxies. Figure 3 shows the integrated fluxes for two neutrino energy regions, $13.3 \leq E_\nu < 17.3$ MeV (low) and $17.3 \leq E_\nu < 31.3$ MeV (high). Here, not only the results from a reference model (GDIMF-wBH) but also those from the alternative models are shown.

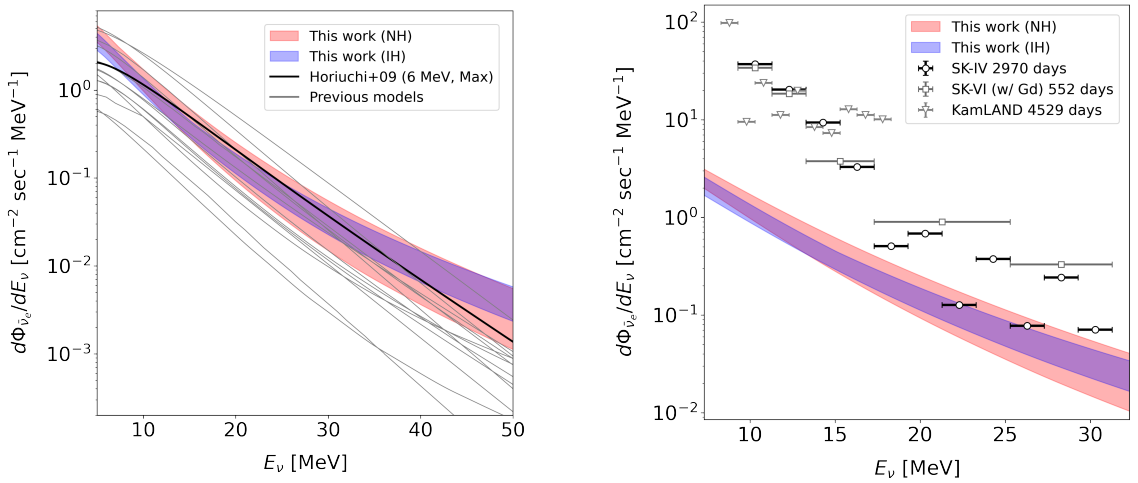

Figure 2: Prediction bands of the DSNB $\bar{\nu}_e$ flux in this work compared with previous theoretical predictions (left) and with the latest experimental upper limits [3, 4, 15] (right). The bands conver different choices of the SFR and nuclear EOS. In the left panel, the prediction from Ref. [16] is highlighted with a solid black line. These figures are taken from Ref. [7].

3. Experimental Detection

Detection of DSNB is achieved mainly via inverse beta decay (IBD) of electron antineutrinos, $\bar{\nu}_e + p \rightarrow e^+ + n$, at water Cherenkov detectors, because of the largest cross section in the MeV regime. The final state positron is detected relatively easily as it emits Cherenkov light directly. On the other hand, the neutron should be converted to γ ray(s) after thermal capture on hydrogen or gadolinium to be detected via Cherenkov light. At water Cherenkov detectors, a combination of these positron and γ ray(s) is required to reduce a huge amount of background events. The event rate spectra at a water volume from the current models are shown in Figure 4.

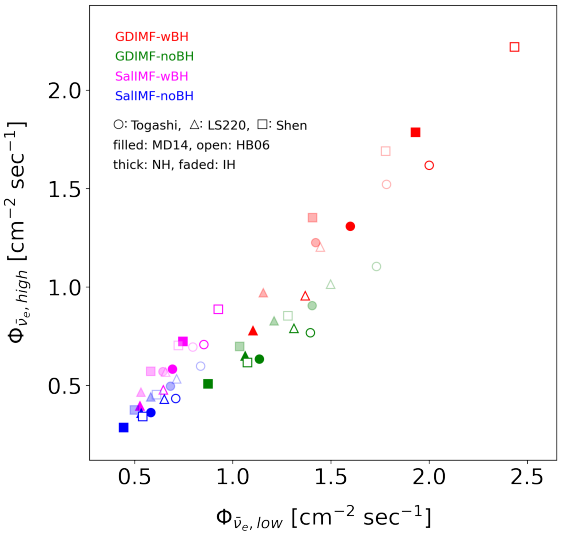

Figure 3: Integrated DSNB $\bar{\nu}_e$ fluxes over the low ($13.3 \leq E_\nu < 17.3$ MeV) and high neutrino energy ranges ($17.3 \leq E_\nu < 31.3$ MeV) for different choices of the IMF, BH treatment, nuclear EOS, SFR, and neutrino mass hierarchy. This figure is taken from Ref. [7].

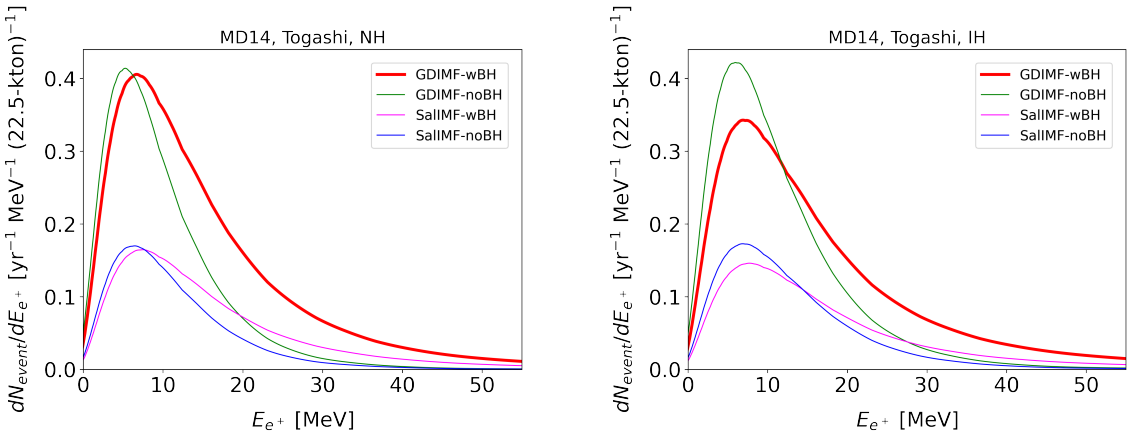

Figure 4: Event rate spectra of the DSNB $\bar{\nu}_e$ at a 22.5 kton water volume for one year with different choices of the IMF and BH treatment for NH (left) and IH (right). Here, MD14 SFR and Togashi EOS are assumed. These figures are taken from Ref. [7].

There are multiple types of background events in the DSNB $\bar{\nu}_e$ search at water Cherenkov detectors: atmospheric neutrinos, spallation isotopes produced from atmospheric muons, solar neutrinos, and reactor neutrinos. Atmospheric neutrinos are known to cause several interactions in water while mainly categorized into neutral-current quasielastic interactions and the others in the context of the DSNB background. Some of energetic muons arriving at a detector break up oxygen nuclei then produce radioactive isotopes in the end, which mimic the DSNB IBD signal. More detailed descriptions about each background can be found in Refs. [3, 5, 7].

In this study, constraints on DSNB models are extracted based on observation inputs with

Bayes' theorem as,

$$P(\text{model}|\text{data}) = \frac{P(\text{data}|\text{model}) \times P(\text{model})}{P(\text{data})} = \frac{P(\text{data}|\text{model}) \times P(\text{model})}{\sum_{\text{model}} P(\text{data}|\text{model}) \times P(\text{model})},$$

where $P(\text{model})$ and $P(\text{data}|\text{model})$ denote a prior and likelihood for a certain model respectively, and $P(\text{model}|\text{data})$ is a posterior with an input data. The sum in the denominator works as a normalization factor which is performed over all models considered in a test. For simplicity, a uniform prior is used in the current analysis. In order to achieve better sensitivity, the number of events in two energy regions, $N_{\text{obs,low}}$ for $13.3 \leq E_\nu < 17.3$ MeV and $N_{\text{obs,high}}$ for $17.3 \leq E_\nu < 31.3$ MeV, are used from an input data, e.g., $\{N_{\text{obs,low}}, N_{\text{obs,high}}\} = \{20, 9\}$ from the fourth operational phase of SK (SK-IV) [3]. In this study, sensitivities at SK-Gd and HK from their 10 years of operations are estimated. Details about analysis setup can be found in Refs. [5, 7].

First, signal strength is investigated by testing the DSNB models against the background-only case. The calculation is repeated for different combinations of SFR, EOS, and neutrino mass hierarchy. The results are shown in Figure 5. Here, the SK-IV results are based on the actual observation from Ref. [3] and the SK-Gd and HK results are obtained by injecting the nominal expectations from each setup as input data. The SK-IV results show a favor of the background-only case while the significance is not high yet. A strong signal claim is found to be possible at SK-Gd and HK. The least significant model is with MD14 SFR, LS220 EOS, and NH because its $N_{\text{obs,low}}$ and $N_{\text{obs,high}}$ are smallest as seen in Figure 3. The posterior probability for this model is largest from the SK-IV data. Secondly, our reference model (GDIMF-wBH) is tested against the alternative models in Table 1 in order to investigate impacts of the assumptions in the model. The calculated results for HK over 10 years are shown in Figure 6. In the case of NH, GDIMF-wBH can be well separated from the others because fluxes in both energy regions are much larger (see the left panel of Figure 4). In contrast, in the case of IH, model separation is more difficult. Novertheless, separation on the IMF assumption (galaxy-dependent or Salpeter) is still feasible (see GDIMF-wBH+GDIMF-noBH vs. SalIMF-wBH+SalIMF-noBH in Figure 6).

In the analysis above, the energy range only between 13.3 and 31.3 MeV is utilized, but it should be noted that the higher and lower energy data can also be useful at future detectors. For example, HK is expected to have enough statistics of data at higher energies. In addition, the liquid scintillation detector such as JUNO can utilize low energy data effectively [17]. The usage of the higher and lower energy data may help to identify the DSNB signal particularly from the present model because of the flux enhancements in these regions (see the left panel of Figure 2).

4. Conclusion

In this study, a variable IMF depending on the galaxy type is introduced and the BH formation is considered for progenitors with $>18M_\odot$ for the DSNB flux calculation. Different combinations of SFR, EOS, and neutrino mass hierarchy are assumed for the calculation. Our new model shows characteristic enhancements at high and low neutrino energies. The enhancement at >30 MeV is explained by a higher rate of the BH formation. On the other hand, the enhancement at <10 MeV is understood by the fact that the core-collapse rate is higher in the early-type galaxies and then more

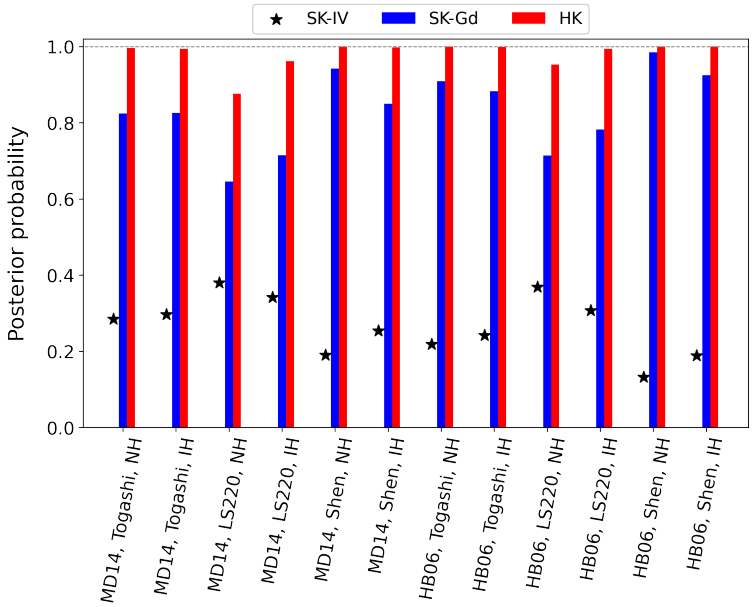

Figure 5: Probabilities of discrimination between the reference DSNB model (GDIMF-wBH) and the background-only case for multiple combinations of SFR, EOS, and neutrino mass hierarchy at different water Cherenkov detectors. This figure is taken from Ref. [7].

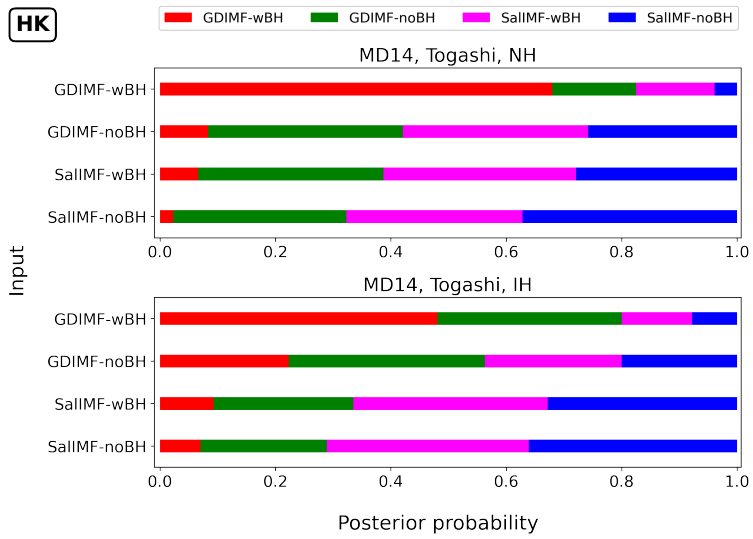

Figure 6: Probabilities of discrimination between the reference and alternative DSNB models with MD14 SFR and Togashi EOS based on HK. This figure is taken from Ref. [7].

neutrinos therein are redshifted. From the test assumed for HK, it is found that DSNB $\bar{\nu}_e$ from the new model can be detected well over the background. In addition, the new model is tested against the alternative models and found to be well discriminated from them at HK.

References

[1] S. Ando, N. Ekanger, S. Horiuchi, and Y. Koshio *arXiv e-prints* (2023) arXiv:2306.16076.

[2] A. M. Suliga *arXiv e-prints* (2022) arXiv:2207.09632.

[3] **Super-Kamiokande** Collaboration, K. Abe *et al.* *Physical Review D* **104** no. 12, (2021) 122002.

[4] **KamLAND** Collaboration, S. Abe *et al.* *The Astrophysical Journal* **925** no. 1, (2022) 14.

[5] Y. Ashida and K. Nakazato *The Astrophysical Journal* **937** no. 1, (2022) 30.

[6] T. Tsujimoto *Monthly Notices of the Royal Astronomical Society* **518** no. 3, (2023) 3475.

[7] Y. Ashida, K. Nakazato, and T. Tsujimoto *arXiv e-prints* (2023) arXiv:2305.13543.

[8] A. M. Hopkins and J. F. Beacom *The Astrophysical Journal* **651** no. 1, (2006) 142.

[9] P. Madau and M. Dickinson *Annual Review of Astronomy and Astrophysics* **52** (2014) 415.

[10] H. Togashi, K. Nakazato, Y. Takehara, S. Yamamuro, H. Suzuki, and M. Takano *Nuclear Physics A,* **961** (2017) 78.

[11] J. M. Lattimer and D. F. Swesty *Nuclear Physics A* **535** no. 2, (1991) 331.

[12] H. Shen, H. Toki, K. Oyamatsu, and K. Sumiyoshi *The Astrophysical Journal Supplement Series* **197** no. 2, (2011) 20.

[13] K. Nakazato, K. Sumiyoshi, and H. Togashi *Publications of the Astronomical Society of Japan* **73** no. 3, (2021) 639.

[14] K. Nakazato, F. Nakanishi, M. Harada, Y. Koshio, Y. Suwa, K. Sumiyoshi, A. Harada, M. Mori, and R. A. Wendell *The Astrophysical Journal* **925** no. 1, (2022) 98.

[15] **Super-Kamiokande** Collaboration, M. Harada *et al.* *arXiv e-prints* (2023) arXiv:2305.05135.

[16] S. Horiuchi, J. F. Beacom, and E. Dwek *Physical Review D* **79** no. 8, (2009) 083013.

[17] **JUNO** Collaboration, A. Abusleme *et al.* *Journal of Cosmology and Astroparticle Physics* **2022** no. 10, (2022) 033.

Acknowledgements

This work is supported by Grant-in-Aid for Scientific Research (JP18H01258, JP20K03973, and JP23H00132) and Grant-in-Aid for Scientific Research on Innovative Areas (JP19H05811) from the Ministry of Education, Culture, Sports, Science and Technology (MEXT), Japan.